Certification of Standard Reference Material® 46h: Fineness of cement - Addition of Blaine and Particle Size Distribution

Chiara F. Ferraris
Max Peltz
Blaza Toman

NIST

**National Institute of
Standards and Technology**

U.S. Department of Commerce

NIST Special Publication 260-190

Certification of Standard Reference Material® 46h: Fineness of cement - Addition of Blaine and Particle Size Distribution

Chiara F. Ferraris
Max Peltz
Materials and Structural Systems Division
Engineering Laboratory

Blaza Toman
Statistical Engineering Division
Information Technology Laboratory

August 2018

U.S. Department of Commerce
Wilbur L. Ross, Jr., Secretary

National Institute of Standards and Technology
Walter Copan, NIST Director and Undersecretary of Commerce for Standards and Technology

Abstract

The standard reference materials (SRM) for fineness of cement are SRM 114 and SRM 46h. They are an integral part of the calibration materials routinely used in the cement industry to qualify cements for ASTM C204 (Blaine), C115 (Wagner) and C430 (45 µm sieve residue). Being a powder, the important physical properties of cement, prior to hydration, are its surface area and particle size distribution (PSD). Since 1934, NIST has provided SRM 114 for cement fineness and it will continue to do so as long as the industry requires it. Subsequent lots of SRM 114 are designated by a unique letter suffix to the SRM number, e.g., 114a, 114b, …, 114q. A certificate provides reference values obtained using ASTM C204 (Blaine), C115 (Wagner) and C430 (45 µm sieve residue) is included with each lot of the material. Since SRM 114p, the certificate also provides the particle size distribution curve by laser diffraction. The current SRM is 114q. In 2007, customers remarked that SRM 114q was too fine to be efficiently used for the C430 calibration. Thus, a new SRM46h was developed by using a coarser cement. This SRM provided values only for C430.

In 2016, both SRM 114q and 46h were tested and the expiration date was extended. However, the stocks for 114q are depleting and it is forecast to be sold out in 2 years to 3 years. Thus, it was decided to certify SRM 46h with ASTM C204 (Blaine), C115 (Wagner) and the particle size distribution (PSD) by laser diffraction. Unfortunately, no data were available for the C115 (Wagner). The stock of 46h is available for another 7years to 8 years.

Thus, an interlaboratory study was organized by NIST to collected data on Blaine and PSD. The data were analyzed to extract the certified value. This report will provide all the data and analysis used to certify SRM 46h for ASTM C204 (Blaine), and the particle size distribution by laser diffraction (AASHTO T253).

Acknowledgements

GCPAT, Inc, Cambridge, Massachusetts; Leslie Buzzell
Hawaii Dept. of Transportation, Honolulu, Hawaii; Brian Ikehara
Heidelberg Technology Center, Doraville, Georgia; Andy Chafin
Holcim (US) Inc., Ada, Oklahoma; Sam Weirick
Hunter Cement Lab, New Braunfels, Texas; Tim Wigley
Illinois Dept of Transportation, Springfield, Illinois; Brian Lokaitis
Kentucky Transportation Cabinet, Frankfort, Kentucky; Wesley Glass
Kosmos, Louisville, Kentucky; Tom Kyser
Lafarge North America, Stoney Creek, Ontario (Canada); Faith Stewart
Lafarge North America, Paulding, Ohio; Jessica Hardenburg
Lafarge North America, Bath, Ontario (Canada); Angelica Marcelo
Lafarge North America, Richmond, British Columbia (Canada); Leila Brooks
Lafarge North America, Pointe Claire, Quebec; Rino Lisella
Lafarge North America, Ravena, New York**;** Peter Cahill
Lehigh Cement, Speed, Indiana; Rebecca Corder
Lehigh Hanson Materials Ltd, Edmonton, Alberta (Canada); Nathan Wannamaker
Lehigh Portland Cem. Co., Leeds, Alabama; Michael U. Reylander
Martin Marietta, Midlothian, Texas; Jeff Wendel
Maryland State Highway Administration, Hanover, Maryland; Vicki R. Stewart
Missouri Dept. of Transp., Jefferson City, Missouri; Chris Bauer
Mitsubishi Cement Corp., Lucerne Valley, California; T. Gepford
Monarch Cement Co., Humboldt, Kansas; Sean Bowman
Montana Department of Transportation, Helena, Montana; Paul Bushnell
Mountain Cement Company, Laramie, Wyoming; Bob Kersey
NH Dept of Transportation Concord, New Hampshire; Richard Fry
NYS Depart of Transportation Labs., Albany, New York; James Simonds
Ohio DOT/Office Mtls Mgmt, Columbus, Ohio; Dan Miller
Oklahoma Dept of Transportation, Oklahoma City, Oklahoma; Danna Crouse
Pennsuco Cement, Medley, Florida; Adriel Oliva
Port Authority of NY & NJ Jersey City, New Jersey; Colin Reed
SC Department of Transportation, Columbia, South Carolina; J.T. Martin
Skyway Cement Company LLC, Chicago, Illinois; Roberto Carrillo
Soil Consultants, Inc., Charleston, South Carolina; Kenny Johnson
St. Mary's Cement, St. Marys, Ontario; April Innes
Vermont Agency of Transportation, Berlin, Vermont; Dustin Hill
WCAN Technical and Development Center, Edmonton, Alberta, Canada; Charla Shain
Wiss, Janney, Elstner Assoc. Inc., Northbrook, Illinois; Ella Shkolnik

Round-Robin Participants for the PSD (Alphabetical)

Alamo Cement Co. 1604 Plant, San Antonio, Texas; Ricardo Rios
Ash Grove Cement Co., Overland Park, Kansas; Chengqing Qi
Argos USA LLC, Calera, Alabama; Nicholas Ewing
Audubon Materials, Sugar Creek, Missouri; Paul Engel
CalPortland, Colton, California; Tom Wilson
Capitol Aggregates, San Antonio, Texas; Doug Conroy
Cemex Tampa Laboratory, Riverview, Florida; Jose Dominguez

Colacem Canada, Grenville Sur La Rouge, Québec (Canada); Mr. Shu Yang
CRH Canada Group, Inc., Mississauga, Ontario (Canada); John Falletta
GCC Rio Grande Pueblo, Pueblo, Colorado; Anne Miller
GCPAT, Inc, Cambridge, Massachusetts; Leslie Buzzell
Heidelberg Technology Center, Doraville, Georgia; Andy Chafin
Lafarge North America, Stoney Creek, Ontario (Canada); Faith Stewart
Lafarge North America, Paulding, Ohio; Jessica Hardenburg
Lafarge North America, Pointe Claire, Quebec; Rino Lisella
Lehigh Hanson Materials Ltd, Edmonton, Alberta (Canada); Nathan Wannamaker
Pennsuco Cement, Medley, Florida; Adriel Oliva
Skyway Cement Company LLC, Chicago, Illinois; Roberto Carrillo

Table of Contents

List of Figures

List of Tables

1. Introduction

A standard reference material (SRM) is a material that has been extensively characterized with regard to its chemical composition, physical properties, or both by NIST. The National Institute of Standards and Technology (NIST) provides over 1300 different SRMs to industry and academia. These certified materials are used in quality assurance programs, for calibration, and to verify the accuracy of experimental procedures. Every NIST SRM is provided with a certificate of analysis that gives the official characterization of the material's properties. In addition, supplementary documentation, such as this report, describing the development, analysis, and use of SRMs, is also often published by NIST to provide the context necessary for effective use of these materials.

There are several SRMs related to cement (https://www.nist.gov/srm). SRM 46h is used to calibrate measurement for the estimation of the fineness of cement, as measured by C430 (45 μm residue). This SRM is the calibration material routinely used in the cement industry to qualify a cement. Being a powder, the main physical properties of cement are its surface area and particle size distribution (PSD). Since 1934, NIST has provided SRM 114 for cement fineness and it will continue to do so as long as the industry requires it. In 2008, the SRM 46h was introduced to respond to customers concerns that SRM 114q was too fine to be useful for calibration using ASTM C430. The SRM 114q has a certificate that gives the values obtained using ASTM C204 (Blaine) [1], C115 (Wagner) [2], C430 (45 μm residue) [3] and measures of the cement particle size distribution (PSD) by laser diffraction are included with each lot of the material. Thus, it was determined that it would be useful to expand SRM 46h with the characterization of the same tests used for SRM 114q. This ensures the supply of a SRM for fineness for the next 7 years to 8 years.

In 1934, only the results of the Wagner test and the 45 μm residue test were listed. In 1944, the Blaine test measurement was added to the SRM 114 certificate. In 2003, the PSD measured by laser diffraction was added as an information value, i.e., not certified. In 2005, the current SRM 114q was released [4, 5], with the certified values for ASTM C204 (Blaine), C115 (Wagner) and C430 (45 μm sieve residue) and the particle size distribution (PSD). The ASTM C115 (Wagner) is no longer used by the industry or at least none of the companies participating in the Cement and Concrete Reference Laboratory (CCRL) Proficiency program.

This report presents the data and statistical analysis to develop the certified values for C204 (Blaine) and particle size distribution for SRM 46h [6]. The values given in this report were obtained through a interlaboratory exercise by volunteer participants from companies participating in the (CCRL) Proficiency program. The development of the PSD in this report was based on the light scattering technology, or as it is commonly referred to, laser diffraction (LD). A discussion on other methods for PSD measurement could be found in ref [7, 8, 9].

2. Description of Method used

2.1 Blaine ASTM C204

The Blaine measurement described in ASTM C204 was adopted by ASTM in 1946. R.L. Blaine published the test in 1943 [10]. The principle of operation is that the permeability of a bed of fine particles is proportional to the fineness of the particles. Therefore, the test is a measurement of the flow rate of air through a bed of cement particles. From the beginning, it was stated that this is a relative test as it depends on the shape of the particles, and the compaction level or porosity of the bed. For this reason, ASTM C204 section 4.1 states that the calibration of the instrument needs to be done by using a reference material, such as SRM 114 [1].

In brief, the test is carried out by packing the cement to be measured in a cell of known volume and placing it on top of a U-tube manometer that contains a non-hygroscopic liquid of low viscosity and density, e.g., dibutyl phthalate or a light grade of mineral oil. The cell is placed on the U-tube in such a way that a tight seal is created and a vacuum is created under the cement cell so that the liquid in the manometer is higher toward the cell. Then, the air is allowed to flow back only through the cement sample. The time for the liquid in the manometer to descend a set distance is measured. This time is used to calculate the fineness quantified by the surface area S of the cement defined using the following formula:

$$S = \frac{S_s \sqrt{T}}{\sqrt{T_s}} \qquad (1)$$

where S is the surface area of the material under test
S_s is the surface area of the reference material, i.e., SRM 114q in this report.
T is the time of flow of the material under test, i.e., SRM 46h
T_s is the time of flow using the reference material, i.e., SRM 114q

Therefore, the surface area of the material tested can be calculated from the reference material by first calculating the correction factor as $S_s / \sqrt{T_s}$

The participants were asked to provide the time of flow measured using first SRM 114q (twice using 1 vial) and then 46h (twice for each of the two vials provided). All participants were requested to measure the SRM 114q material immediately before measuring the SRM 46h material and to report all results.

2.2 Laser Diffraction

Laser diffraction measurements can be performed with the powder either dispersed in air or in a liquid. From the data received for this study, the dispersion in air is more common

2

and participant reported using both techniques. A very brief description of laser diffraction methods is presented, with discussion on the principles of operation, the range of application, the key parameters, and the requirements for sample preparation and their potential impact on the measurement results.

The laser diffraction (LD) [11] method involves the detection and analysis of the angular distribution of light produced by a laser beam passing through a dilute dispersion of particles. Typically, a He-Ne laser (wavelength $\lambda = 632.8$ nm) in the 5 mW to 10 mW range is employed as the coherent light source, but more recently solid-state diode lasers have come into use and provide a range of available wavelengths in the visible and UV spectrum. Since the focal volume of the beam senses many particles simultaneously, and thus provides an average value, it is referred to as an *ensemble* technique. With the exception of single particle optical scattering (SPOS), all scattering methods are ensemble techniques, and only ensemble methods will be considered here. There are a number of different diffraction and scattering phenomena that can be utilized for particle sizing. Likewise, there are a number of different ways to define and classify these methods, depending on the underlying principle or its application. We have chosen to classify all time-averaged scattering and diffraction phenomena involving laser optics, under the general heading of laser diffraction; however, it should be noted that "laser diffraction" is often used in a narrower way to refer to techniques that utilize only low-angle scattering. See ref [12] for a list of equivalent or related methods.

One can differentiate among light waves that are *scattered*, *diffracted* or *absorbed* by the dispersed particles. The scattered light consists of reflected and refracted waves, and depends on the form, size, and composition of the particles. The diffracted light arises from edge phenomena, and is dependent only on the geometric shadow created by each particle in the light beam path: diffraction is therefore independent of the composition of the particles. In the case of absorption, light waves are removed from the incident beam and converted to heat or electrical energy by interaction with the particles; absorption depends on both size and composition.

The influence of composition is controlled by the complex refractive index, $m = n - ik$, where $i = \sqrt{-1}$. For non-absorbing (i.e., transparent) particles, $k = 0$, where k, the imaginary component of the refractive index, is related to the absorption coefficient of the material. Both the real part of the refractive index, n, and the imaginary part, k, are wavelength-dependent. Scattering arises due to differences in the refractive index of the particle and the surrounding medium (or internal variations in heterogeneous particles). Therefore, to use a scattering model to calculate the PSD that produced a specific scattering pattern, one must first know the complex refractive index of both the particles and the medium (typically, a medium is selected that has an imaginary component value of k=0). Values of n have been published for many bulk materials [13], but in the case of cement, n is routinely estimated based on a mass average of the refractive indices for the individual material components [14] and its value was fixed at 1.7 for all round-robins [7, 8] and in this report. The imaginary refractive component is more difficult to determine and/or find in the published literature [15, 16], and this often represents a significant challenge to the use of scattering methods for fine particle size measurements [17].

3

As a general rule of thumb, the darker or more colored a specimen appears, the higher the imaginary component. For white powders, such as high-purity alumina, $k=0$. Cement, on the other hand, is generally gray to off-white in color, and therefore one can anticipate a finite, but relatively low value for the imaginary component. $k = 1$ was fixed for cement in this round-robin, although this value is unverified and will likely vary for different formulations. In the literature, the value of $k=0.1$ is also often used for cement. Further studies are needed to determine the correct value.

Mie theory, which describes scattering by homogeneous spheres of arbitrary size, is the most rigorous scattering model available, and is used in many commercial instruments. For non-spherical particles like cement, Mie theory provides a volume-weighted equivalent spherical diameter. Mie theory has been applied with mixed success to the analysis of fine powders with diameters from several hundredth of micrometers down to several tenths of micrometers. An accurate representation of the "true" size distribution by Mie scattering is dependent on a knowledge of the complex refractive index, and will be impacted by the degree of asymmetry present in the particles and the dispersion procedure used to prepare the test sample. The Mie approach does not work well for extremely fine particulates with sizes below 100 nm, possibly because of increased sensitivity to uncertainties in the refractive index that occur with these materials. Hackley et al. [11] determined the range of value of the refractive indices for cement.

For very large particles (relative to the wavelength of the light used [11]), the diffraction effect can be exploited without reference to Mie theory or the complex index of refraction. Diffracted light is concentrated in the forward direction, forming the so-called Fraunhofer diffraction rings. The intensity and distribution of diffracted light around the central beam can be related to particle size, again assuming spherical geometry. The validity for this method is limited, on the low end, to particle diameters a few times greater than the wavelength of the incident light for particles that are opaque or have a large refractive index contrast with the medium [18]. For near transparent particles, or particle with a moderate refractive contrast, the lower limit is increased to about 40 times the wavelength of light. For a He-Ne laser, this corresponds to about 25 μm. The benefit of using Fraunhofer diffraction is that the interpretation is not dependent on the absorptive or refractive properties of the material. A totally absorbing black powder, a translucent glass powder, and a highly reflective white powder, having the same particle size and shape, will produce identical Fraunhofer patterns within the valid size range. On the other hand, inappropriate use of the Fraunhofer approximation outside of the valid range can lead to large systematic errors in the calculated PSD [14, 19]. These errors are especially prevalent in the size range below one micrometer, where errors exceeding 100 % are possible. Partial transparency can lead to the appearance of "ghost" particles, generally in the size range below one micrometer, produced as an artifact of the refractive dispersion of light within the transparent particles. The refracted light is registered at large scattering angles as anomalous diffraction, and is therefore interpreted by the Fraunhofer analysis as being produced by very small particles.

4

In general, the LD method requires that the particles be dispersed, either in liquid (suspension) or in air (aerosol). The former is commonly referred to as the "wet" method (LD-W) while the latter is termed the "dry" method (LD-D). In Fraunhofer diffraction, the pattern does not depend on the refractive index, so there is no theoretical difference between using a liquid or a gas as a dispersing medium as long as the particles are equally well dispersed. For Mie scattering, the higher refractive index contrast in air, compared with most liquids, may impact the scattering pattern, without altering the results.

Differences between LD-D and LD-W methods arise primarily from the different ways in which the particles are dispersed in each case. In liquid, it is possible to modify solution conditions, e.g., by changing pH or adding chemical dispersing agents, or to break up aggregates using mechanical or ultrasonic energy. Thus, in general, a better state of dispersion can be achieved in a properly selected liquid medium, i.e., a liquid not chemically reactive with the powder and with a different refractive index than the powder. For silicates and most metal oxides, water is an excellent dispersing medium. However, due to the reactive nature of cement in water, alcohols, such as isopropanol, methanol, and ethanol, are commonly used instead. In the LD-D method, a stream of compressed air (or a vacuum) is used to both disperse the particles and to transport them to the sensing zone. This method of dispersion works well for large, non-colloidal-phase spheroids, where the interfacial contact area is small and the physical bonds holding the individual particles together are relatively weak. For particles smaller than one micrometer and highly asymmetric, the higher surface-to-volume ratio results in more intimate and numerous contact points and, as a consequence, a greater driving force is needed to separate aggregated particles.

3. Materials

The cement selected and its characterization can be found in the original reports related to SRM 114q [4, 5] 46h [6]. The material used for this study was already packaged as both SRMs are available from NIST. Vials (not whole units containing 10 vials) were randomly selected and shipped to the participating laboratories.

4. Data analysis for the Blaine qualification

4.1 Data received

NIST received the data from a total of 68 laboratories. 51 laboratories provided the time in seconds as requested and 17 laboratories calculated the Blaine values. It is expected that the latter used a calibration factor developed earlier and not using the SRM 114q provided. The 51 laboratories that provided the time [s] were analyzed at NIST (Appendix A, Table A.1) in two steps: *1*) the correction factor was calculated using equation (1) and the SRM 114q data from the certificate and *2*) the Blaine of the SRM 46h was calculate using the factor obtained under point *1*. SRM 114q is certified for Blaine as 381.8 m²/kg ± 7.8 m²/kg, where the uncertainty is the expanded uncertainty (95%).

4.1.1 Statistical analysis of the Blaine Calculated from time measurements (51 Labs)

The statistical analysis described here computes Blaine value based on the 51 labs that provided the time measurements.

The Blaine values were computed using the following statistical model, based on an observation equation [23], and incorporating a Gaussian random effects model [24], which represents this calibration procedure, and includes all known sources of uncertainty:

$B_{114q} \sim N(381.8, 3.9^2)$, the random variable representing the certified SRM 114q Blaine
> *Note: The SRM 114q certificate has Blaine as 381.8 m²/kg with expanded uncertainty of 7.8 m²/kg. So, 3.9 is half of that because this is the standard uncertainty.*

$s_{1_{ij}} \sim N\left(\left(\frac{B_{114q}}{F_i}\right)^2, \sigma_i^2\right), i = 1,\dots,51, \ j = 1,2$ are the time measurements for SRM 114q for lab i,

$s_{2_{ij}} \sim N\left(\left(\frac{b_{46hs_i}}{F_i}\right)^2, \sigma_i^2\right), i = 1,\dots,51, \ j = 1,\dots,4$ are the time measurements for SRM 46h for lab i,

$b_{46hs_i} \sim N(B_{46h}, \sigma_T^2), i = 1,\dots,51$.

The measurand is the Blaine value for SRM 46h denoted by B_{46h}. The uncertainty of this value accounts for variability in measurements $s_{1_{ij}}$ (this is the within lab uncertainty σ_i), measurements $s_{2_{ij}}$, and b_{46h_i} (between lab uncertainty σ_T). Evaluation was done via Markov Chain Monte Carlo method [25], using the OpenBUGS [26] code in the Appendix.

Using this model, the Blaine of SRM 46h, B_{46h}, has mean 364.4 m^2/kg with standard uncertainty of 2.59 m^2/kg and 95% uncertainty interval of (359.3 m^2/g, 369.7 m^2/g).

4.1.2 Statistical analysis of the Blaine provided (15 labs)

The data set consisted of 15 sets of Blaine values, two replicated measurements $x_{1_{ij}}$ for SRM 114q and four replicates $x_{2_{ij}}$ for SRM 46h. Using the certified value of SRM 114q [21] B_{114q}, we can adjust the Blaine SRM 46h measurements of each lab by a factor that corrects for an under or over estimate that was observed in their SRM 114q measurements. The model of the calibration ($\tilde{x}_2$ is the adjusted SRM 46h value) is as follows:

$$G = \frac{B_{114q}}{x_1}$$

$$\tilde{x}_2 = G \times x_2$$

The following statistical model, again based on an observation equation, and a Gaussian random effects model, will do that:

$x_{1_{ij}} \sim N\left(\left(\frac{B_{114q}}{G_i}\right), \sigma_{xi}^2\right), i = 1,\dots,17, j = 1,2$ are the Blaine measurements for SRM 114q for lab i,

$x_{2_{ij}} \sim N\left(\left(\frac{b_{46hx_i}}{G_i}\right), \sigma_{xi}^2\right), i = 1,\dots,17, j = 1,\dots,4$ are the Blaine measurements for SRM 46h for lab i,

$b_{46hx_i} \sim N(B_{46h}, \sigma_B^2), i = 1,\dots,17$.

Using this model Blaine of SRM 46h, B_{46h}, has mean 364.2 m^2/kg with standard uncertainty of 4.82 m^2/kg and 95% uncertainty interval of (354.8 m^2/kg, 373.7 m^2/kg).

4.1.3 Combined estimate of Blaine.

The calculated and direct measurements of Blaine are combined using both statistical models together. The obtained B_{46h} mean is 364.4 m^2/kg with standard uncertainty of 2.68 m^2/kg and 95 % uncertainty interval of (359.1 m^2/kg, 369.7 m^2/kg).

5. Data Analysis for Laser Diffraction

5.1 Laser diffraction parameters

In this round-robin, the participants were free to use either method (LD-W or LD-D), but they had to respond to a questionnaire (Appendix C) and some parameters were fixed. They were also asked to follow AASHTO T353-14 [20].

The fixed parameters were:
- Cement Refractive index: 1.7
- Cement Imaginary index: 1
- In LD-W: Isopropanol was requested and the refractive index of isopropanol was set to be 1.39.

The responses to the questionnaire are summarized in Table 1 and Table 2. It can be noticed that some participants did not return the questionnaire and some elected not to use the refractive indices requested. None were excluded, as outliers were declared by comparison of the other data. The influence of the refractive indices on the particle size distribution was studied in ref [11].

Table 1: Parameters reported by participants for LD-W

Lab #	Refractive index			Normal Medium[a]	Concentration of cement in the medium[b]	Dilution from stock	Ultra sound			LD Measurement Duration [sec]	Model (M/F/B)[d]
	Real	Imag.	Medium				Y/N	Duration[c]	Where		
94	1.52	0.1	1.33	IPA		No	N		Prior to Device (dilute suspension)	4	N/A
126	1.7	1	1.39	IPA	99.9 g/ mL	No	Y	Intensity 6/ 30 s	Inside	60	F
343											
605	1.7	1	1.39	IPA	Unknown	No	Y	40 W/ 50 s	Inside	30	M
1079	1.7	1	1.39	IPA		No	Y	35 W/60 s	Inside	180	B

Notes:

[a]: The participants were requested to use IPA but they were also asked if this was the alcohol that they normally use. If not they were asked to indicate what alcohol they used normally. Therefore, this column gives the name of the alcohol that they normally use.

[b]: The concentration of cement is reported here as given by the participants. The units are as given by the participant. They are given here for information only.

[c]: The intensity of the ultrasound is reported here as given by the participants. The units are as given by the device and they are device/manufacturer dependent. Therefore, they cannot be converted to fundamental units. They are given here for information only.

[d] : The participants were asked to state the model that they used to interpret the data: M= Mie; F= Fraunhofer; B=both

Table 2: Parameters reported by participants for LD-D

Lab #	Refractive Index		Air pressure [bar]	Measurement duration [s]	Model (M/F/B)[#]	Comments[+]
	Real	Imag.				
142	1.7	1	Not reported	45	M	
156	1.7	1	Not reported	90	M	
178	1.68	1	4		M	
180	1.7	1	4.0	10	M	
219	1.7	1	Vacuum	10	M	
255	1.7	1	6.7	60	M	Needed to use 2 vials or 12g for each PSD to achieve the correct transmission number
309	1.7	1	Vacuum	17	M	
504						
1323	1.7	1	2.5	12	M	
2491	1.7	1	6	70		
2522	1.5	1	3.875	12	B	
2763	1.7	1	4	12	M	
3255	1.7	1	2	10 (see note)	F	Measurement duration: 10 s or when the optical concentration drops below 1 % Range (1.8 to 350) μm

Note:

: The participants were asked to state the model that they used to interpret their data: M= Mie; F= Fraunhofer; B=both

+: The comments are as reported by the participants. They refer on how the cement to be tested was treated before the measurement.

6. Analysis of the Particle Size Distribution Data

6.1 Introduction

Each participant was provided with 1 vial of SRM 114q and 2 vials of SRM 46h to test. They were asked to perform 3 runs on each vial. The data were transmitted in a standard spreadsheet. The average of the three runs for each vial was calculated and then the data were reduced, for simplification of data interpretation, to a cumulative particle size distribution with the following sizes: (1, 1.5, 2, 3, 4, 6, 8, 12, 16, 24, 32, 48, 64, 96, 128) μm. All data are shown in Appendix D. Each participant laboratory is identified by their CCRL number in this report.

There were 13 participants who provided data with LD-D (68 %) and 6 with LD-W (32 %). These participants represent 28 % of the laboratories that participated in the round-robin for the Blaine (Section 4). Nevertheless, the participation was sufficient for statistical analysis, allowing calculation of mean particle size distribution for the two cements (SRM 114q and SRM 46h) with the uncertainty (Section 6.4).

6.2 Data for SRM 114q

All the participants curves are shown in Figure 1 and Figure 2 for the LD-D and LD-W respectively.
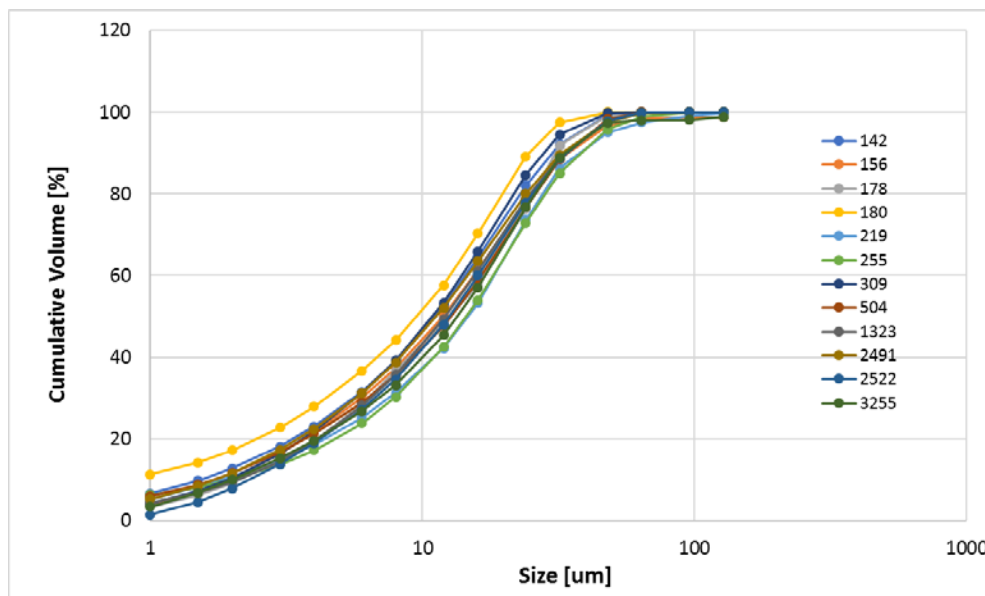
Figure 1: LD-D for SRM 114q for each laboratory identified by the CCRL number. Each curve is the average of 3 replicates. Uncertainty, calculated as the standard deviation of the 3 measurements results on an individual laboratory is smaller than the symbol.
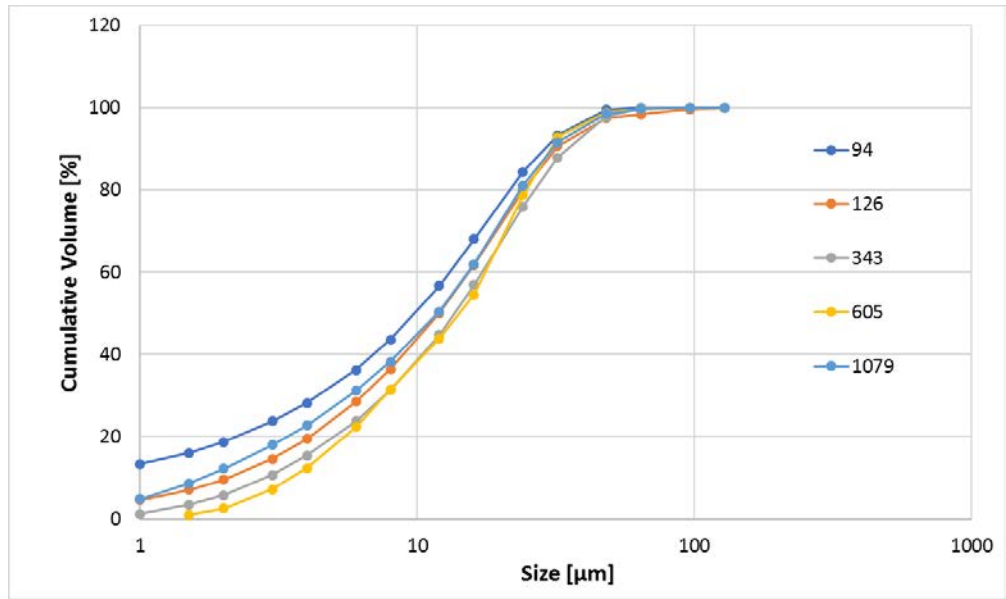
Figure 2: LD-W for SRM 114q for each laboratory identified by the CCRL number. Each curve is the average of 3 replicates. Uncertainty, calculated as the standard deviation of the 3 measurements results on an individual laboratory is smaller than the symbol.

6.3 Data for SRM 46h

All the curves obtained are shown in Figure 3 and 4. No outliers were identified. However, lab 619 was not used in the analyses because data for only a single replicate was reported.
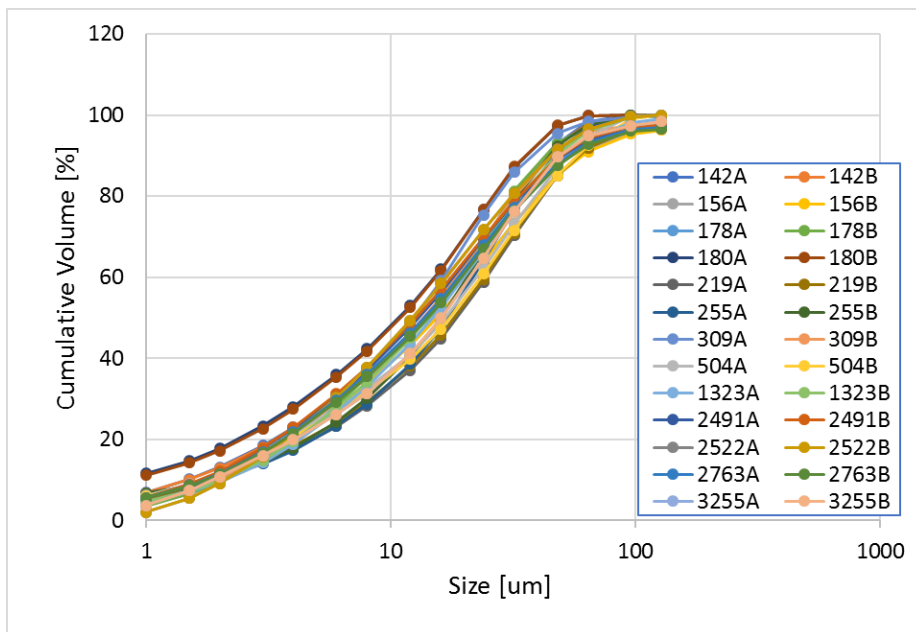
Figure 3: LD-D for SRM 46h for each laboratory identified by the CCRL number. Each curve is the average of 3 replicates. The letters A or B stand for each of the 2 vials used by each laboratory. Uncertainty, calculated as the standard deviation of the 3 measurements results on an individual laboratory is smaller than the symbol.
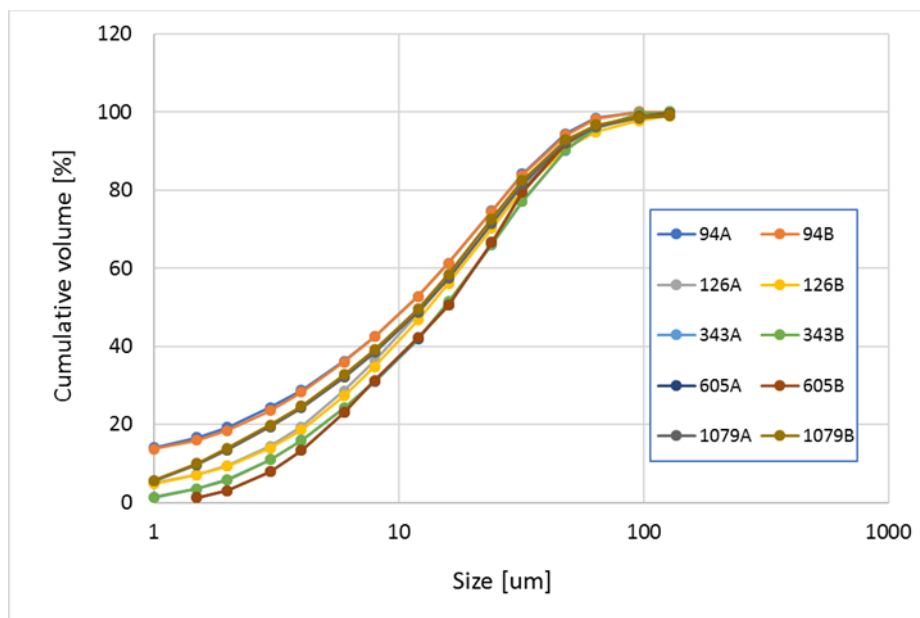
Figure 4: LD-W for SRM 46h for each laboratory identified by the CCRL number. Each curve is the average of 3 replicates. The letters ABC stand for each of the 3 vials used by each laboratory. Uncertainty, calculated as the standard deviation of the 3 measurements results on an individual laboratory is smaller than the symbol.

6.4 Statistical analysis of the data for PSD

Among the 17 laboratories reporting, twelve that measured dry and five that measured wet. The same laboratories also measured SRM 114q using the same method that they used for SRM 46h. The statistical analysis proceeded by first transforming the data back to a frequency table form. This made it possible to employ the multinomial probability distribution to obtain a set of consensuses estimates of the multinomial proportions, together with their uncertainty and simultaneous confidence bounds. These were then transformed back into the cumulative density form. The OpenBUGS code for the computations is given in the Appendix.

Since for both the dry and the wet data sets, there were some apparent outlying laboratories, the analysis was done with and without the outliers.

6.4.1 Analysis of LD-D results

All the data received from the labs that measured SRM 46h using LD-D are analyzed here. Figure 3 and Figure 5 show all the data received. It seems clear from Figure 5 that the labs 180 and 255 are outliers. Figure 6 also show that the same labs are outliers in the measurements of SRM 114q.

Table 3: SRM 46h LD-D cumulative analysis of all the labs (including outliers)

Particle Size [μm]	Mean Cumulative [%]	95 % uncertainty		95 % predictive interval	
		Lower	Upper	Lower	Upper
1	5.27	4.35	6.19	0.58	9.99
1.5	8.25	7.30	9.18	3.43	13.12
2	11.15	10.2	12.11	6.24	16.09
3	16.42	15.43	17.42	11.32	21.63
4	20.93	19.89	21.96	15.68	26.30
6	28.42	27.32	29.53	22.75	34.13
8	34.57	33.45	35.73	28.61	40.52
12	44.63	43.44	45.85	38.32	50.95
16	53.16	51.94	54.41	46.81	59.68
24	67.38	66.09	68.72	60.76	74.18
32	78.05	76.65	79.48	71.00	85.53
48	90.16	88.63	91.71	82.58	98.22
64	95.34	93.72	96.98	87.21	100
96	98.36	96.63	100	89.65	100
128	98.82	97.08	100	90.07	100
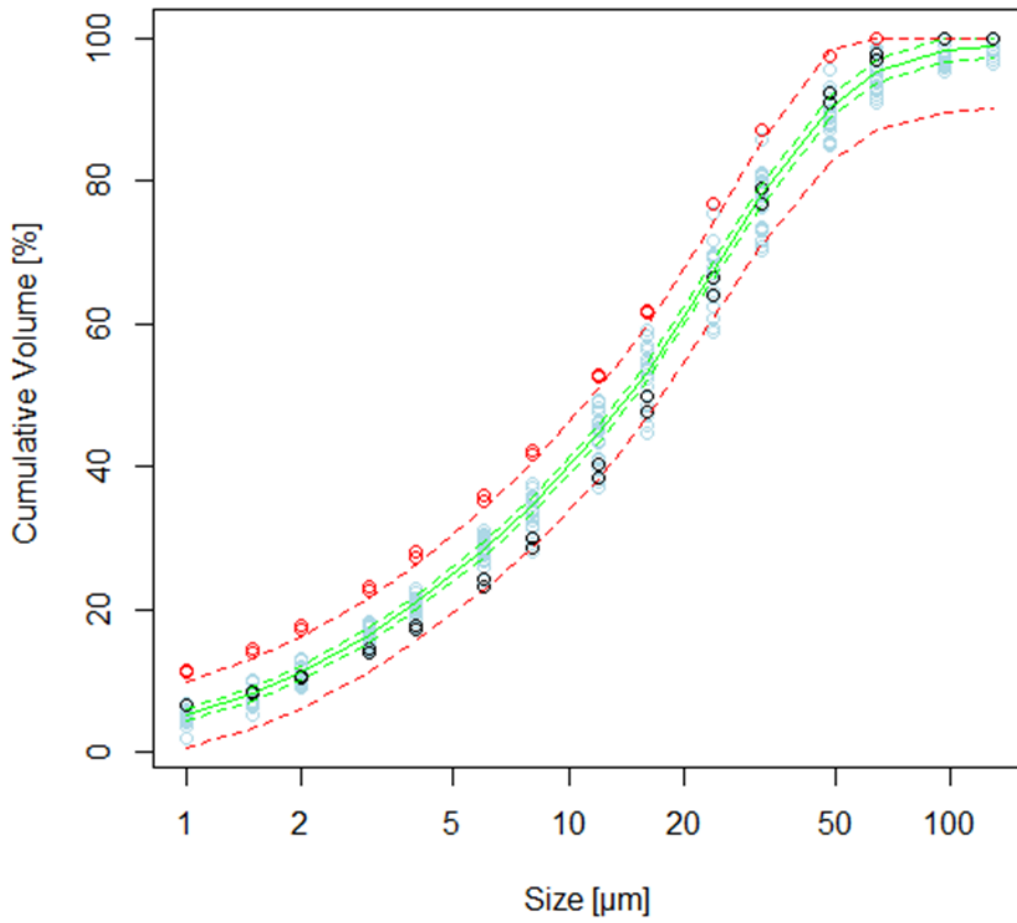
Figure 5: Measurements in blue (outlier labs: #180 in red, #255 in black), 95 % uncertainty bound in green, 95 % predictive bound in red.
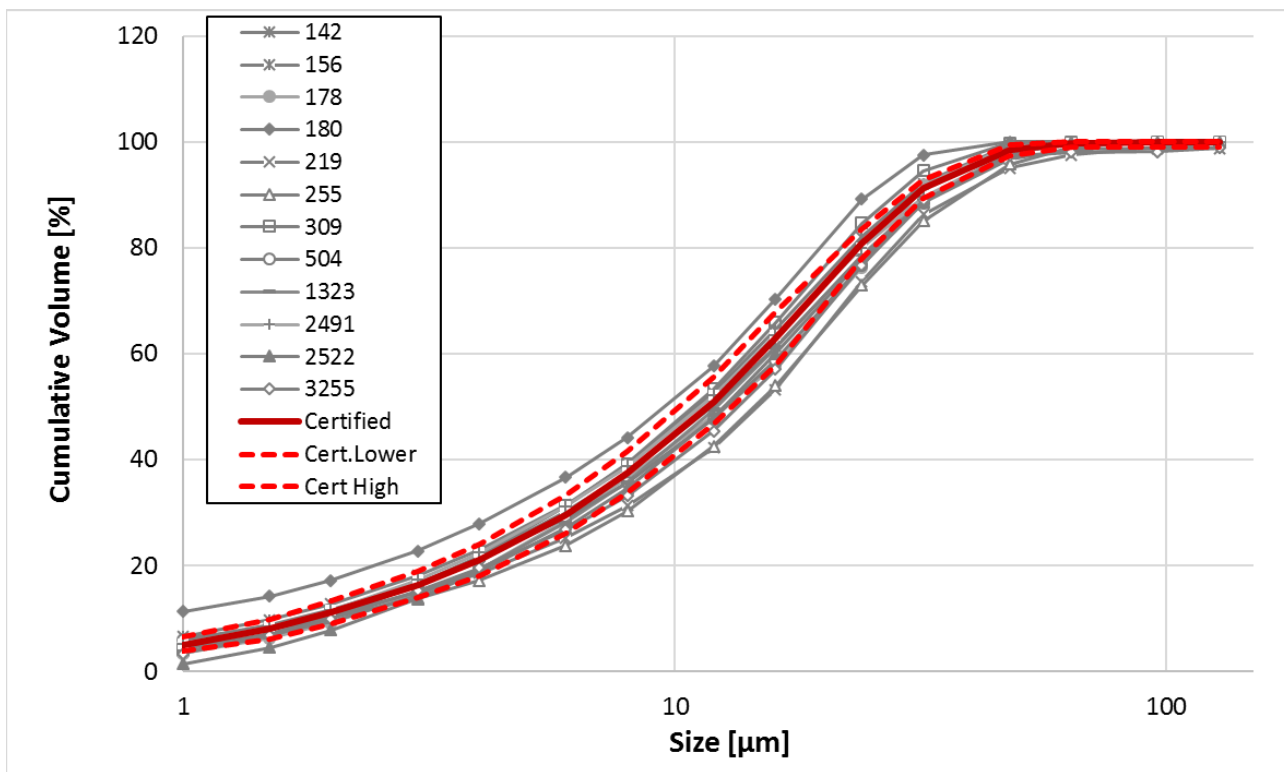
Figure 6: SRM 114q LD-D measurements with the certified values. Same data from Figure 1 with the addition of the certified values

Table 4: SRM 46h LD-D cumulative analysis of all the labs (without the outliers- labs 180 & 255)

Particle Size [μm]	Mean Cumulative [%]	95 % uncertainty		95 % predictive interval	
		Lower	Upper	Lower	Upper
1	4.59	4.00	5.20	1.67	7.57
1.5	7.67	7.06	8.29	4.69	10.70
2	10.63	10.00	11.28	7.55	13.71
3	16.03	15.34	16.72	12.62	19.40
4	20.61	19.87	21.36	17.02	24.23
6	28.19	27.31	29.04	24.01	32.44
8	34.36	33.40	35.30	29.80	39.01
12	44.36	43.32	45.40	39.30	49.42
16	52.78	51.71	53.86	47.56	58.01
24	66.74	65.60	67.91	61.10	72.33
32	77.26	75.95	78.56	71.13	83.36
48	89.37	87.93	90.80	82.63	96.32
64	94.76	93.25	96.27	87.52	100.00
96	98.08	96.45	99.69	90.47	100.00
128	98.61	96.96	100.00	90.84	100.00

18
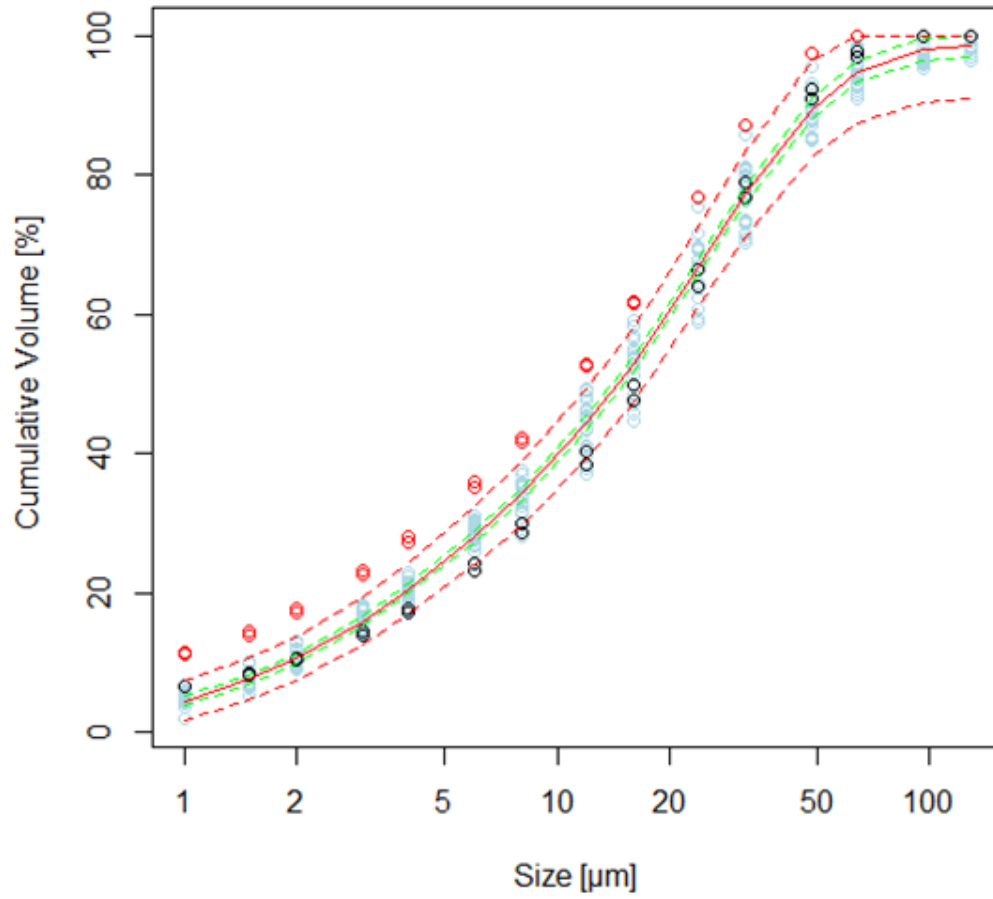
Figure 7. Measurements in blue (outlier labs: #180 in red, #255 in black), estimates made without labs 180 and 255, 95 % uncertainty bound in green, 95 % predictive bound in red.

6.4.2 Analysis of LD-W results

All the data received from the labs that measured SRM 46h using LD-W are analyzed here. Table 5 and Figure 8 show all the data received. It seems clear from Figure 8 that the labs 94 and 605 are outliers. Figure 8 also show that the same labs are outliers in the measurements of SRM 114q.

Table 5: Values for SRM 46h by LD-W (All data received)

Particle Size [μm]	Mean Cumulative [%]	95% uncertainty		95% predictive interval	
		Lower	Upper	Lower	Upper
1	6.45	2.47	10.51	0.00	19.10
1.5	9.24	5.18	13.39	0.00	22.06
2	11.97	7.89	16.15	0.00	24.66
3	17.20	13.08	21.39	4.98	29.99
4	21.98	17.84	26.16	9.83	34.75
6	30.20	26.07	34.42	17.94	43.07
8	36.97	32.78	41.28	24.58	50.08
12	47.85	43.61	52.15	35.41	61.04
16	56.84	52.59	61.13	44.33	70.03
24	70.92	66.71	75.25	58.26	84.04
32	80.91	76.65	85.33	68.06	94.14
48	92.12	87.71	96.67	78.58	100
64	96.58	92.14	100	82.76	100
96	99.16	94.70	100	85.32	100
128	99.65	95.17	100	85.70	100
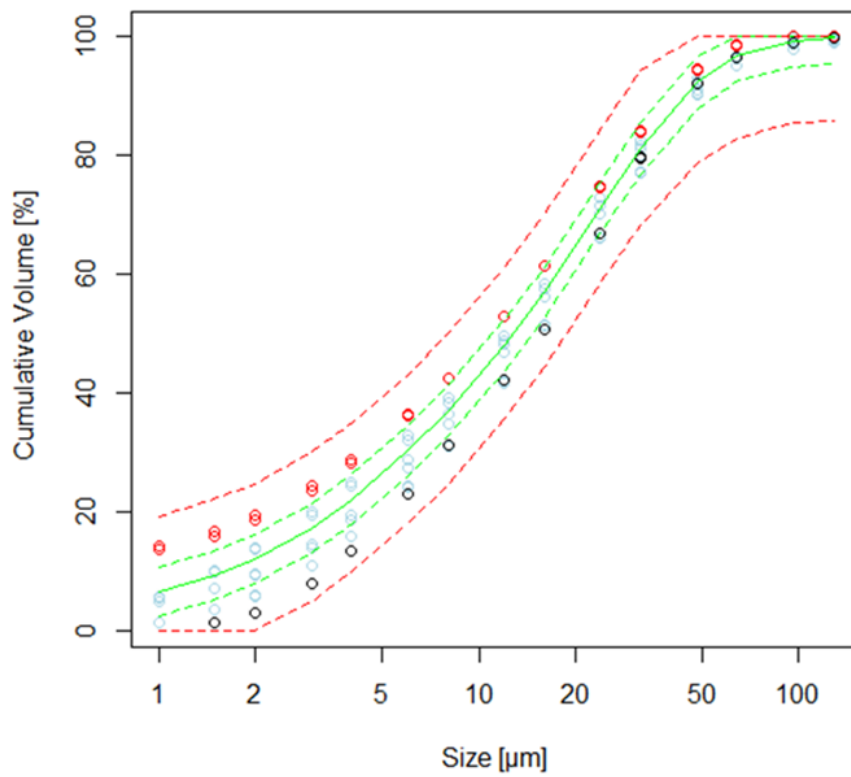
Figure 8: All Measurements for 46h using LD-W (blue o). Lab 94 is in red, and lab 605 is in black. The average data and 95 % uncertainty bound are in green, while the 95 % predictive bound are in red.
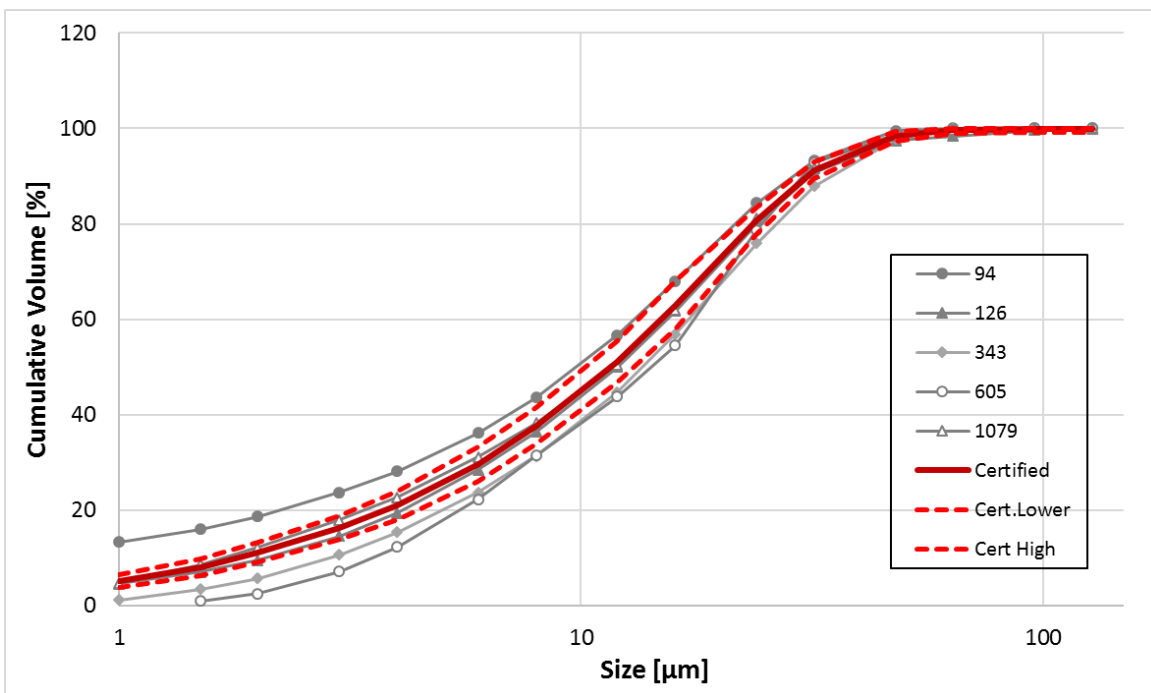
Figure 9: SRM 114q measurements by LD-W with the certified values from the certificate. Same values as shown in Figure 2 with the addition of the certified values.

Table 6: SRM 46h by LD-W excluding the outliers (labs 94 and 605)

Particle Size [μm]	Mean Cumulative [%]	95% uncertainty		95% predictive interval	
		Lower	Upper	Lower	Upper
1	3.95	1.80	6.09	0.00	9.786
1.5	6.86	4.46	9.27	0.37	13.34
2	9.64	7.10	12.20	2.59	16.57
3	14.93	12.35	17.57	7.81	21.98
4	19.79	17.2	22.43	12.59	26.93
6	28.2	25.56	30.92	20.84	35.46
8	35.13	32.46	37.93	27.62	42.55
12	46.18	43.36	49.05	38.42	53.88
16	55.35	52.52	58.26	47.52	63.15
24	69.67	66.79	72.61	61.78	77.46
32	79.89	76.92	82.88	71.88	87.98
48	91.4	88.16	94.69	82.52	100
64	95.99	92.62	99.4	86.64	100
96	98.89	95.47	100	89.36	100
128	99.54	96.13	100	90.06	100
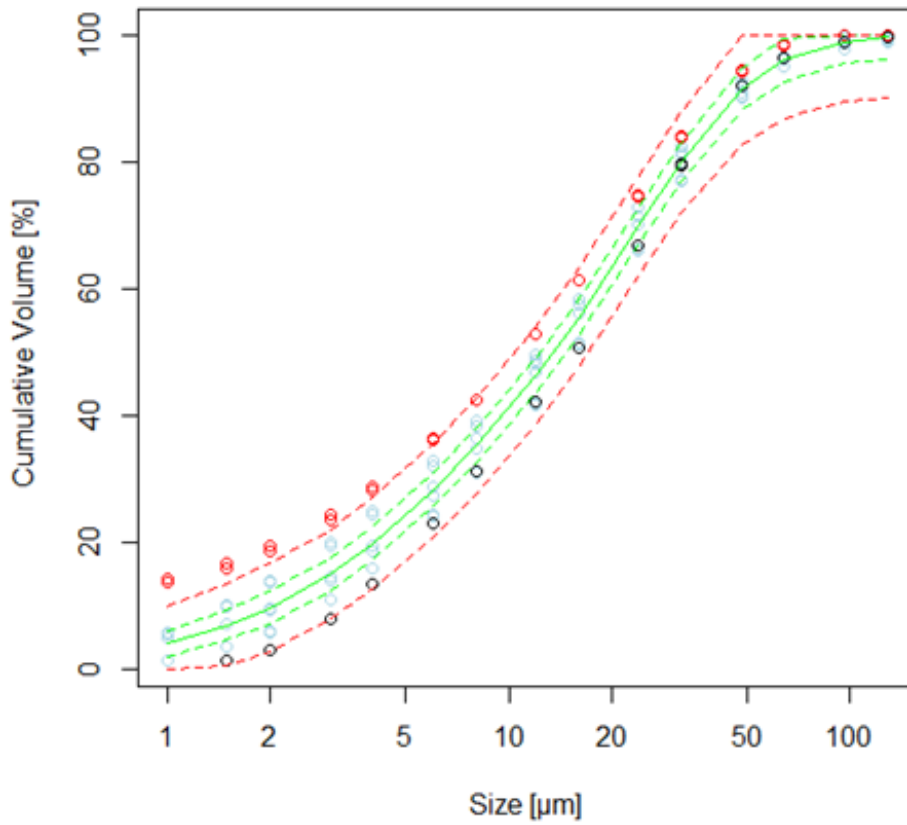
Figure 10. All Measurements for 46h using LD-D (blue o). The outlies are lab 94 in red, and lab 605 in black. The average data and 95 % uncertainty bound are in green, while the 95 % predictive bound in red.

6.5 Combining both LD-W and LD-D data for SRM 46h

Figure 11 shows the measurement curves for both LD-D and LD-W for SRM 46h.
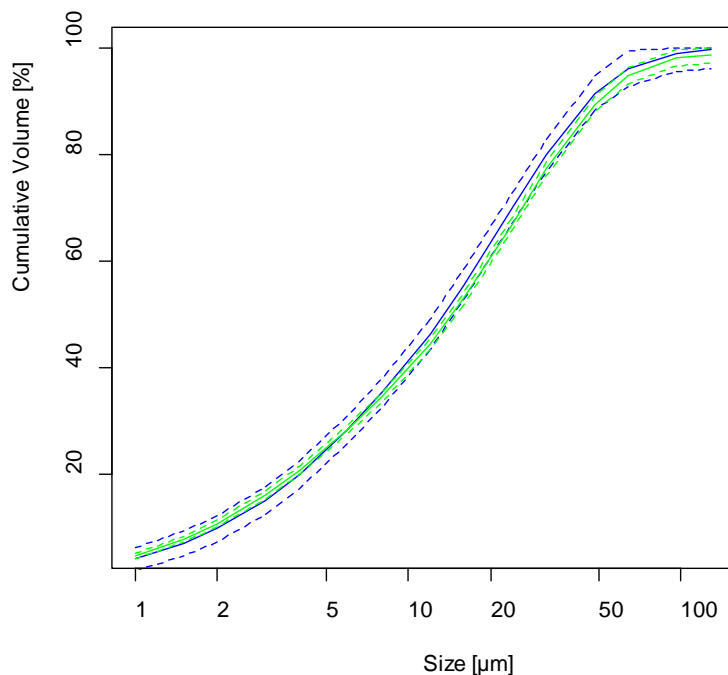
Figure 11: Mean cumulative volume with 95 % uncertainty bounds for LD-D in green and LD-W in blue.

The results for the dry method are more precise because there are more laboratories that use this method. To further compare, the following table gives the differences between the cumulative volume in % obtained by the dry method and by the wet method, together with the 95 % uncertainty bounds. The table shows that two methods produce the same cumulative volume within their 95 % uncertainty bounds.

As the methods are comparable, it is sensible to combine their results to produce an estimate of the cumulative volume in % given in Table 7.

Table 7: Differences between the cumulative volume in % obtained by the LD-D and LD-W method.

Particle Size [μm]	Difference in %	Lower 95 % interval for the difference in %	Upper 95 % interval for the difference in %
1	0.67	-1.57	2.79
1.5	0.84	-1.65	3.25
2	1.01	-1.62	3.59
3	1.12	-1.59	3.75
4	0.84	-1.87	3.49
6	0.00	-2.84	2.79
8	-0.76	-3.69	2.09
12	-1.80	-4.87	1.19
16	-2.55	-5.64	0.47
24	-2.90	-6.06	0.19
32	-2.61	-5.82	0.61
48	-2.00	-5.51	1.58
64	-1.20	-4.93	2.51
96	-0.77	-4.59	3.04
128	-0.89	-4.73	2.92

Table 8: Combination of 46H data both LD-D and LD-W without the ouliers

Particle Size [μm]	Mean Cumulative [%]	95 % uncertainty		95 % predictive interval	
		Lower	Upper	Lower	Upper
1	4.5	3.95	5.08	1.8	7.2
1.5	7.6	7.02	8.17	4.7	10.4
2	10.5	9.945	11.14	7.6	13.5
3	15.9	15.26	16.56	12.7	19.2
4	20.7	19.96	21.34	17.2	24.1
6	28.5	27.72	29.36	24.3	32.7
8	34.9	34.00	35.84	30.4	39.5
12	45.1	44.14	46.17	40.1	50.2
16	53.8	52.69	54.85	48.5	59.1
24	67.9	66.78	69.02	62.3	73.5
32	78.3	77.10	79.46	72.0	84.5
48	90.2	88.94	91.57	83.3	97.1
64	95.4	94.05	96.84	88.1	100
96	98.6	97.11	100	90.9	100
128	99.1	97.68	100	91.4	100
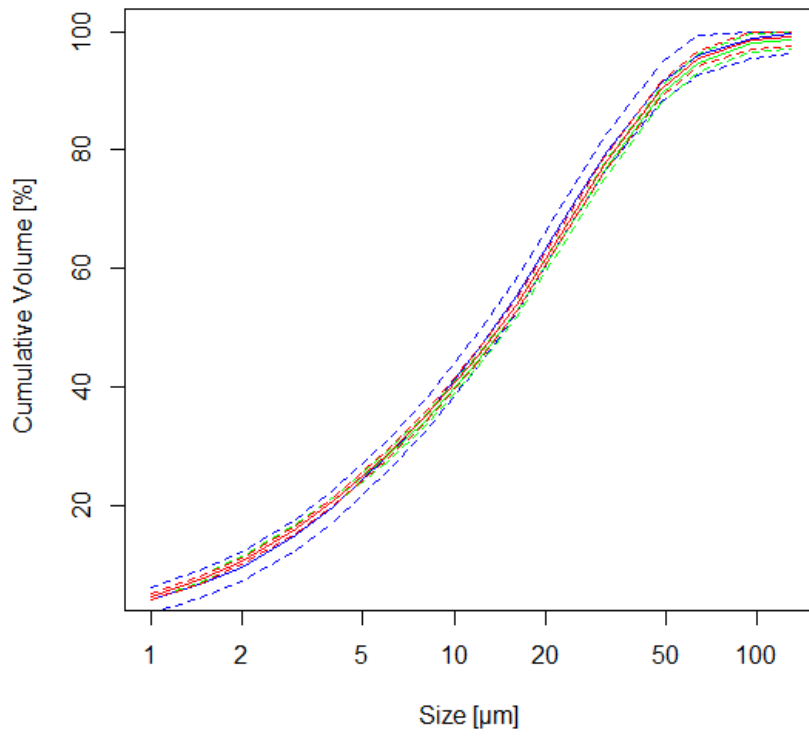
Figure 12: Mean cumulative volume with 95 % uncertainty bounds for LD-D in green, LD-W in blue, and the combined estimate in red.

7. Summary

7.1 Blaine Value for 46h

The consensus Blaine value is 364.4 m^2/Kg with standard uncertainty of 2.68 m^2/kg and 95% uncertainty interval of (359.1 m^2/kg, 369.7 m^2/kg). This value will be reported on the certificate.

7.2 The PSD for SRM 46h

The SRM 114q particle size distribution (PSD) was determined using laser diffraction (LD) techniques in a round-robin evaluation. The values were measured by volunteer participants from companies participating in the CCRL proficiency program. These laboratories run these measurements routinely. Two LD methods were included in the tests: LD-D, in which the powder was measured in a dry dispersed state as an aerosol (dry) and LD-W, in which the powder was dispersed in a non-aqueous liquid medium (wet). The parameters requested for the lab to use are:

- The real part of the complex refractive index was 1.7 and the imaginary part was 1.0 for both methods
- For LD-W: IPA was used as the medium and the refractive index used for IPA was 1.39 (imaginary = 0).

The differences between the results from these two methods were not found to be statistically significant, so that data from both methods were combined and used to calculate the mean particle size distribution, shown graphically in Figure 12 and in tabulated in Table 8. This particle size distribution could be used as a reference to validate methodology and instrument operation as described in Section 5. It should be made clear that the uncertainty values shown in Table 8 are intended to represent how well the SRM 46h size distribution is known at this time. Therefore, it is not expected that all the participant laboratories data would fall within these boundaries. The 95% predictive intervals include between laboratory uncertainty and so should include most of the laboratories data. The uncertainty between laboratories and within laboratories is discussed in Section 6.4.
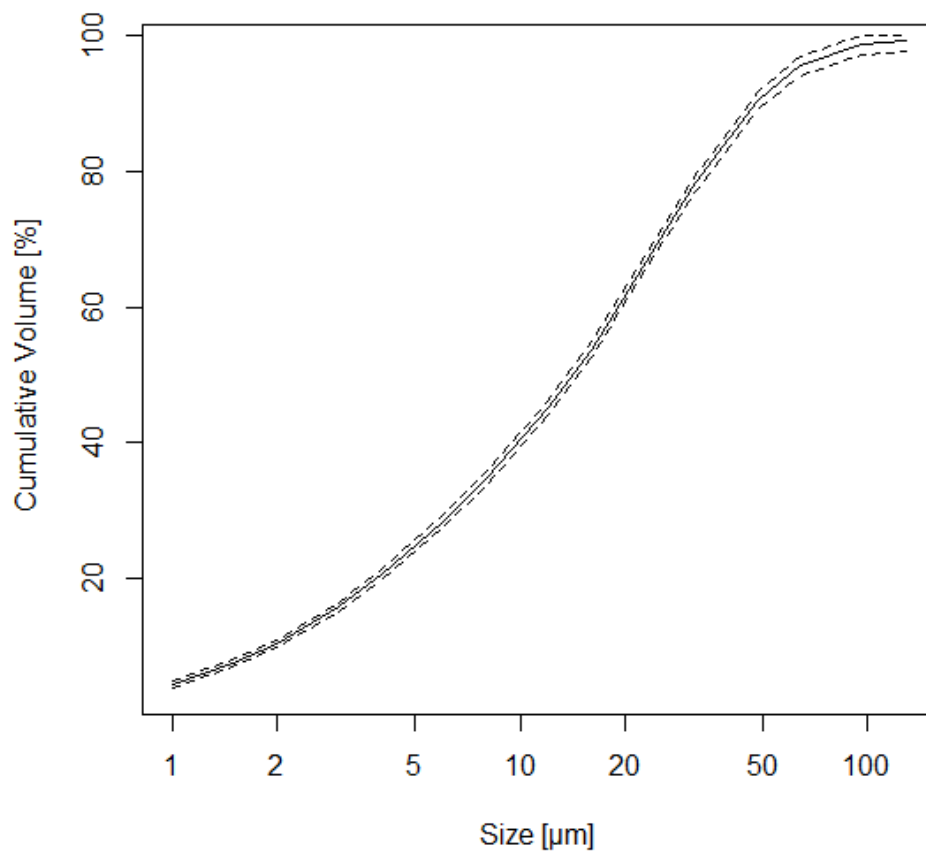
Figure 13 : Combined PSD by LD of SRM 46h (extracted from Figure 12)

Table 8: Particle size distribution for SRM 46h using LD (combined wet and dry).

Particle Size [μm]	Mean Cumulative [%]	95 % uncertainty	
		Lower	Upper
1	4.5	3.95	5.08
1.5	7.6	7.02	8.17
2	10.5	9.945	11.14
3	15.9	15.26	16.56
4	20.7	19.96	21.34
6	28.5	27.72	29.36
8	34.9	34.00	35.84
12	45.1	44.14	46.17
16	53.8	52.69	54.85
24	67.9	66.78	69.02
32	78.3	77.10	79.46
48	90.2	88.94	91.57
64	95.4	94.05	96.84
96	98.6	97.11	100
128	99.1	97.68	100

8. References

1. "Standard Test Method for Fineness of Hydraulic Cement by Air Permeability Apparatus", ASTM C204-00 Volume: 04.01

2. "Standard Test Method for Fineness of Portland Cement by the Turbidimeter", ASTM C115-96a (2003) Volume: 04.01

3. "Standard Test Method for Fineness of Hydraulic Cement by the 45-µm (No. 325) Sieve", ASTM C430-96 (2003) Volume: 04.01

4. Ferraris, C.F., Guthrie W., Avilés A.I., Haupt, R., B. McDonald "Certification of SRM 114q; Part I", NIST SP260-161, July 2005

5. Ferraris C.F., Guthrie W., Ivelisse Avilés A., Peltz M., Haupt R., MacDonald B. S. "Certification of SRM 114q; Part II (Particle Size distribution)", NIST SP260-166, November 2006

6. Ferraris C.F., Guthrie W., Peltz M., Haupt R., "Certification of SRM 46H" NIST SP-260-169, January 2008

7. Ferraris, C.F, Hackley V.A., Aviles A.I., Buchanan C.E., "Analysis of the ASTM Round-Robin Test on Particle Size Distribution of Portland Cement: Phase I" NISTIR 6883, May 2002 (http://ciks.cbt.nist.gov/monograph, Part I, chapter 3, section 8a)

8. Ferraris, C.F, Hackley V.A., Aviles A.I., Buchanan C.E., "Analysis of the ASTM Round-Robin Test on Particle Size Distribution of Portland Cement: Phase II" NISTIR 6931, December 2002 (http://ciks.cbt.nist.gov/monograph, Part I, chapter 3, section 8b)

9. Ferraris C.F., Hackley V.A., Avilés A.I., "Measurement of Particle Size Distribution in Portland Cement Powder: Analysis of ASTM Round-Robin Studies", Cement, Concrete and Aggregate Journal, Dec. 2004, vol. 26 #2, pp 71-81

10. Blaine R.L., "A simplified air permeability fineness apparatus" - ASTM Bull, 1943

11. Hackley V., Lum L-S., Gintautas V., Ferraris C., "Particle Size Analysis by Laser Diffraction Spectrometry: Applications to Cementitious Powders", NISTIR 7097, March 2004.

12. Jillavenkatesa A., Dapkunas S. J., Lum L.-S. H., Particle Size Characterization, NIST Special publication 960-1, 2001.

13. Handbook of Optical Constants of Solids, edited by E.D. Palik, Academic Press, New York, 1985; Handbook of Optical Constants of Solids II, edited by E.D. Palik, Academic Press, New York, 1991.

14. Cyr M. and Tagnit-Hamou A., "Particle size distribution of fine powders by laser diffraction spectrometry. Case of cementitious materials," *Materials and Structures*, **34**, 342-350 (2000).

15. Lindberg J.D., Douglass R.E. and Garvey D.M., "Absorption-coefficient-determination method for particulate materials," *Applied Optics*, **33**[9], 4314-4319 (1994).

16. Marley N.A., Gaffney J.S., Baird J.C., Blazer C.A., Drayton P.J. and Frederick J.E., "An empirical method for the determination of the complex refractive index of size-

fractionated atmospheric aerosols for radiative transfer calculations," *Aerosol Science and Technology*, **34**, 535-549 (2001).

17. Bohren C.F. and Huffman D. R., "Absorption and Scattering of Light by Small Particles", John Wiley & Sons, New York, 1983.

18. ISO 13320-1:1999(E), Particle size analysis — LASER diffraction methods — Part 1: General principles.

19. Seville J.P.K., Coury J.R., Ghadiri M., and Clift R., "Comparison of techniques for measuring the size of fine non-spherical particles," Particle Characterization, **1**, 45-52 (1984).

20. AASHTO T 353-14: "Standard Method of Test for Particle Size Analysis of Hydraulic Cement and Related Materials by Light Scattering",

21. SRM 114q Certificate: https://srmors.nist.gov/certificates/view_cert2gif.cfm?certificate=114q   Or by selecting "Standard Reference Materials" from the website www.NIST.GOV and typing in 114p

22. Montgomery D. C., *Design and Analysis of Experiments*, 2nd Edition, John Wiley and Sons, New York, 1984.

23. Possolo A., Toman B. (2007) Assessment of measurement uncertainty via observation equations, Metrologia 44:464–475.

24. Toman B., Possolo A. (2009) Laboratory effects models for interlaboratory comparisons, Accred Qual Assur 14:553 563.

25. Casella G., Berger R.L. (2002). Statistical Inference, 2nd ed. Duxbury Press.

26. Lunn D.J., Spiegelhalter D., Thomas A., Best N. (2009) The BUGS project: Evolution, critique, and future directions, Statistics in Medicine 28:3049–3082.

Appendix A: Data for Blaine

Table A.1: Blaine obtained from time measurements provided (51 laboratories)

CCRL code	Time measurement [s] 114q		46h sample #1		46h sample #2		Factors based on 114q Meas 1	Meas 2	Aver.	St. dev	Calculated Blaine [m²/g] 114q		46h sample #1		46h sample #2	
N43	89.3	91.0	82.2	83.3	82.0	83.9	40.4	40.0	40.2	0.3	380.0	383.6	364.4	367.0	364.0	368.4
N2	98.1	98.8	86.9	86.6	87.1	87.4	38.5	38.4	38.5	0.1	381.1	382.5	358.8	358.2	359.1	359.7
N3	376.0	375.0	369.0	373.0	375.0		19.7	19.7	19.7	0.0	382.1	381.5	378.5	380.5	381.5	
N68	93.2	93.2	88.3	88.4	88.5	88.5	39.5	39.5	39.5	0.0	381.8	381.8	371.6	371.8	372.0	372.0
N50	88.0	88.0	81.0	81.0	81.0	81.0	40.7	40.7	40.7	0.0	381.8	381.8	366.3	366.3	366.3	366.3
N64	111.2	112.1	100.0	101.1	99.6	100.5	36.2	36.1	36.1	0.1	381.0	382.6	361.3	363.3	360.6	362.2
N29	67.0	68.0	60.0	60.0	62.0	62.0	46.6	46.3	46.5	0.2	380.4	383.2	360.0	360.0	365.9	365.9
1	81.9	80.2	88.0	87.4	84.0	87.8	42.2	42.6	42.4	0.3	383.8	379.8	397.8	396.5	388.7	397.4
4	95.0	96.0	85.0	86.5	86.0	86.0	39.2	39.0	39.1	0.1	380.8	382.8	360.2	363.4	362.3	362.3
15	71.0	72.0	86.0	74.0	78.0	70.0	45.3	45.0	45.2	0.2	380.5	383.1	418.7	388.4	398.8	377.8
17	95.5	93.3	83.8	81.5	83.5	81.0	39.1	39.5	39.3	0.3	384.1	379.6	359.7	354.7	359.0	353.7
20	95.6	95.2	89.5	86.6	90.6	88.4	39.0	39.1	39.1	0.1	382.2	381.4	369.8	363.6	372.0	367.5
28	93.1	93.0	84.8	84.6	83.6	83.4	39.6	39.6	39.6	0.0	381.9	381.7	364.5	364.1	361.9	361.5
30	94.0	92.0	88.0	88.0	87.0	87.0	39.4	39.8	39.6	0.3	383.9	379.8	371.4	371.4	369.3	369.3
35	135.9	138.2	127.7	126.2	127.4	126.2	32.8	32.5	32.6	0.2	380.2	383.4	368.6	366.4	368.1	366.4
36	80.5	80.1	77.9	80.9	81.0	80.4	42.6	42.7	42.6	0.1	382.2	381.4	376.1	383.3	383.4	382.0
46	96.0	93.0	81.0	81.0	83.0	83.0	39.0	39.6	39.3	0.4	384.9	378.8	353.5	353.5	357.8	357.8
50	94.9	94.9	86.3	84.6	86.5	84.7	39.2	39.2	39.2	0.0	381.8	381.8	364.1	360.5	364.4	360.8
70	106.9	106.7	97.6	97.5	97.5	97.2	36.9	37.0	36.9	0.0	382.0	381.6	365.0	364.8	364.8	364.2
94	78.9	78.8	70.3	69.5	70.0	68.6	43.0	43.0	43.0	0.0	381.9	381.7	360.4	358.5	359.6	356.1
101	119.2	119.0	106.1	105.9	106.5	105.9	35.0	35.0	35.0	0.0	382.0	381.6	360.4	360.0	361.0	360.0
129	83.0	82.0	80.0	80.0	80.0	80.0	41.9	42.2	42.0	0.2	383.0	380.6	376.0	376.0	376.0	376.0

CCRL code	Time measurement [s]						Factors based on 114q				Calculated Blaine					
	114q		46h sample #1		46h sample #2		Meas. 1	Meas. 2	Aver.	St. dev	114q		46h sample #1		46h sample #2	
131	114.9	114.4	106.9	107.9	110.4	110.2	35.6	35.7	35.7	0.1	382.2	381.4	368.7	370.4	374.7	374.3
142	90.6	91.6	81.5	80.7	82.2	81.0	40.1	39.9	40.0	0.2	380.8	382.9	361.1	359.4	362.7	360.0
152	92.3	92.5	80.0	80.3	80.3	80.3	39.7	39.7	39.7	0.0	381.6	382.0	355.3	355.9	355.9	355.9
156	103.0	103.0	92.0	91.0	92.0	90.0	37.6	37.6	37.6	0.0	381.8	381.8	360.8	358.9	360.8	356.9
167	149.5	149.1	132.0	132.3	132.1	132.7	31.2	31.3	31.2	0.0	382.1	381.5	359.0	359.4	359.1	359.9
177	87.0	88.5	75.0	76.0	75.5	77.0	40.9	40.6	40.8	0.2	380.2	383.4	353.0	355.3	354.2	357.7
178	93.1	94.2	83.4	81.8	83.6	84.8	39.6	39.3	39.5	0.2	380.7	382.9	360.3	356.8	360.7	363.3
180	111.2	112.1	67.2	68.2	68.3	69.3	36.2	36.1	36.1	0.1	381.0	382.6	296.2	298.4	298.6	300.8
254	91.0	91.6	86.5	85.9	83.6	84.1	40.0	39.9	40.0	0.1	381.2	382.4	371.6	370.4	365.2	366.4
255	87.8	85.2	76.1	74.9	71.8	77.5	40.7	41.4	41.1	0.4	384.7	379.0	358.1	355.3	347.9	361.4
294	105.9	106.3	91.6	92.4	93.5	93.1	37.1	37.0	37.1	0.0	381.4	382.2	354.8	356.3	358.4	357.6
309	103.7	101.1	96.5	97.2	97.5	96.2	37.5	38.0	37.7	0.3	384.2	379.4	370.6	372.0	372.6	370.0
343	109.8	108.0	101.0	97.3	100.4	98.5	36.4	36.7	36.6	0.2	383.4	380.2	367.7	360.9	366.6	363.1
413	90.0	90.0	79.0	78.0	79.0	80.0	40.2	40.2	40.2	0.0	381.8	381.8	357.7	355.4	357.7	360.0
441	97.0	104.0	93.0	95.0	93.0	93.5	38.8	37.4	38.1	0.9	375.3	388.6	367.4	371.4	367.4	368.4
474	39.3	37.3	31.3	31.7	30.7	31.7	60.9	62.5	61.7	1.1	386.8	376.9	345.3	347.1	341.6	347.1
504	94.9	95.4	90.8	89.2	90.0	89.8	39.2	39.1	39.1	0.1	381.3	382.3	372.8	369.7	371.3	370.9
515	87.0	85.5	84.4	84.3	90.7		40.9	41.3	41.1	0.3	383.5	380.1	377.7	377.5	391.6	
605	107.2	105.8	95.6	96.5	99.0	96.4	36.9	37.1	37.0	0.2	383.1	380.5	361.7	363.4	368.1	363.3
611	117.4	116.6	115.2	115.5	113.6	114.7	35.2	35.4	35.3	0.1	382.5	381.1	378.9	379.3	376.2	378.0
687	93.2	92.0	84.5	83.1	82.5	83.2	39.6	39.8	39.7	0.2	383.1	380.5	364.9	361.9	360.4	362.0
840	81.0	79.0	69.0	71.0	71.0	73.0	42.4	43.0	42.7	0.4	384.2	379.4	354.6	359.7	359.7	364.7
1079	93.3	92.1	83.1	82.9	83.1	83.5	39.5	39.8	39.7	0.2	383.0	380.6	361.4	361.0	361.5	362.5
1323	104.8	101.8	95.1	92.1	91.7	91.9	37.3	37.9	37.6	0.4	384.7	379.0	366.3	360.6	359.7	360.1
1435	119.0	118.0	107.0	106.0	107.0	104.0	35.0	35.1	35.1	0.1	382.6	381.0	362.8	361.1	362.8	357.7
1726	87.0	88.0	89.0	90.0	88.0	89.0	40.9	40.7	40.8	0.2	380.7	382.9	385.1	387.2	382.9	385.1
1819	71.0	72.0	63.0	64.0	65.0	64.0	45.3	45.0	45.2	0.2	380.5	383.1	358.4	361.2	364.0	361.2
2522	100.2	99.6	88.9	88.1	87.2	87.6	38.1	38.3	38.2	0.1	382.4	381.2	360.2	358.5	356.7	357.5
3255	119.6	119.2	104.9	106.5	105.0	103.9	34.9	35.0	34.9	0.0	382.1	381.5	357.9	360.6	358.0	356.2

Table A.2: Blaine provided by the laboratories (17 Laboratories)

CCRL code	Blaine [m²/g] 114q		46h sample #1		46h sample #2	
7	381.8	382.3	365.2	364.0	363.1	362.0
10	396.0	376.0	403.6	407.3	407.4	406.4
90	381.8	383.9	371.0	366.7	355.4	373.2
93	391.0	387.0	362.0	367.0	359.0	362.0
105	384.6	380.4	352.9	355.6	358.4	358.7
125	397.8	400.0	377.1	377.1	374.8	379.5
126	379.0	380.0	363.0	359.0	363.0	363.0
159	383.0	387.7	361.1	361.1	358.6	363.6
165	379.4	380.6	360.6	354.0	360.2	364.4
205	373.3	373.6	354.0	353.6	353.3	355.3
219	368.2	368.2	349.9		352.0	358.2
354	373.0	371.0	353.0	352.0	355.0	352.0
431	384.0	384.0	368.6	368.6	368.6	366.4
457	385.7	383.8	361.6	359.5	359.5	360.5
501	383.0	383.0	360.0	361.0	360.0	360.0
1594	381.0	382.0	365.0	363.0	363.0	363.0
2491	382.0	382.0	368.0	369.0	368.0	368.0

Appendix B: Statistical analysis for Blaine

The following code performs the statistical analysis from 4.1.3 using Markov Chain Monte Carlo in OpenBUGS. The Blaine estimate based on both calculated (based on time) and direct measurements is called "Blainem". Its posterior mean is the certified value and its posterior standard deviation and 95 % posterior probability region are the certified standard uncertainty and the certified 95 % uncertainty interval.

OpenBUGS code:

```
This code produces the estimate of Blaine (Blainem) based on all data.
{s114~dnorm(381.8,0.066)
cut.s<-cut(s114)
 ## estimates based on the time measurements
xiNs ~ dnorm(0, 0.0016)I(0.001,)
            chSqNs~ dgamma(0.5,0.5)
            sigl <- xiNs/sqrt(chSqNs)
Blainem~dunif(300,500)
for(i in 1:53){xiNsb[i] ~ dnorm(0, 0.0016)I(0.001,)
            chSqNsb[i] ~ dgamma(0.5,0.5)
            sig[i] <- xiNsb[i]/sqrt(chSqNsb[i])
            fact[i]~dunif(0,100)
            Blaine[i]~dnorm(Blainem,sigl)
            m[1,i]<-(cut.s/fact[i])*(cut.s/fact[i])
cut.fact[i]<-cut(fact[i])
            m[2,i]<-(Blaine[i]/cut.fact[i])*(Blaine[i]/cut.fact[i])}
for(i in 1:316){meas[i]~dnorm(m[material[i],lab[i]],sig[lab[i]])}
##
## estimates based on the direct measurements

BxiNs ~ dnorm(0, 0.0016)I(0.001,)
            BchSqNs~ dgamma(0.5,0.5)
            sigB<- BxiNs/sqrt(BchSqNs)
xiNs2 ~ dnorm(0, 0.0016)I(0.001,)
            chSqNs2~ dgamma(0.5,0.5)
            sig2<- xiNs2/sqrt(chSqNs2)
xiNs3 ~ dnorm(0, 0.0016)I(0.001,)
            chSqNs3~ dgamma(0.5,0.5)
            sig3<- xiNs3/sqrt(chSqNs3)

for (i in 1:15){G[i]~dunif(0.6,1.6)
            m114[i]<-(cut.s/G[i])
cut.G[i]<-cut(G[i])
            Blained[i]~dnorm(Blainem,sigB)
            mean[i]<-(Blained[i]/cut.G[i]) }

for(i in 1:30){meas114[i]~dnorm(m114[lab3[i]],sig3)}

for(i in 1:59){meas2[i]~dnorm(mean[lab2[i]],sig2)}
}
```

Data:

Set 1:

lab is the laboratory identification for the time measurement,

meas is the time measurement

material = 1 is the SRM 114q measurement,

material = 2 is the SRM 46h measurement

lab[]	meas[]	material[]
1	81.9	1
1	80.2	1
1	88	2
1	87.4	2
1	84	2
1	87.8	2

35

2	71	1
2	72	1
2	86	2
2	74	2
2	78	2
2	70	2
3	103	1
3	103	1
3	92	2
3	91	2
3	92	2
3	90	2
4	87	1
4	85.47	1
4	84.4	2
4	84.29	2
4	90.72	2
5	119	1
5	118	1
5	107	2
5	106	2
5	107	2
5	104	2
6	87	1
6	88.5	1
6	75	2
6	76	2
6	75.5	2
6	77	2
7	93.1	1
7	94.2	1
7	83.4	2
7	81.8	2
7	83.6	2
7	84.8	2
8	96	1
8	93	1
8	81	2
8	81	2
8	83	2
8	83	2
9	107.2	1
9	105.8	1
9	95.6	2
9	96.5	2
9	99	2
9	96.4	2
10	90	1
10	90	1
10	79	2
10	78	2
10	79	2
10	80	2
11	92.3	1
11	92.5	1
11	80	2
11	80.3	2
11	80.3	2
11	80.3	2
12	81	1
12	79	1
12	69	2
12	71	2
12	71	2
12	73	2
13	91.01	1
13	91.58	1
13	86.48	2
13	85.93	2
13	83.55	2
13	84.09	2
14	149.5	1
14	149.1	1
14	132	2
14	132.3	2
14	132.1	2
14	132.7	2

15	78.9	1
15	78.81	1
15	70.27	2
15	69.52	2
15	69.96	2
15	68.61	2
16	90.6	1
16	91.6	1
16	81.5	2
16	80.7	2
16	82.2	2
16	81	2
17	100.2	1
17	99.6	1
17	88.9	2
17	88.1	2
17	87.2	2
17	87.6	2
18	105.9	1
18	106.3	1
18	91.6	2
18	92.4	2
18	93.5	2
18	93.1	2
19	119.2	1
19	119	1
19	106.1	2
19	105.9	2
19	106.5	2
19	105.9	2
20	87.8	1
20	85.2	1
20	76.1	2
20	74.9	2
20	71.8	2
20	77.5	2
21	89.3	1
21	91.03	1
21	82.15	2
21	83.31	2
21	81.95	2
21	83.92	2
22	119.6	1
22	119.2	1
22	104.9	2
22	106.5	2
22	105	2
22	103.9	2
23	111.2	1
23	112.1	1
23	67.2	2
23	68.2	2
23	68.3	2
23	69.3	2
24	95.54	1
24	93.32	1
24	83.82	2
24	81.5	2
24	83.47	2
24	81.02	2
25	93.28	1
25	92.1	1
25	83.07	2
25	82.883	2
25	83.08	2
25	83.533	2
26	93.17	1
26	91.95	1
26	84.53	2
26	83.14	2
26	82.45	2
26	83.22	2
27	98.1	1
27	98.79	1
27	86.94	2
27	86.64	2
27	87.1	2

27	87.4	2
28	80.47	1
28	80.11	1
28	77.91	2
28	80.91	2
28	80.95	2
28	80.39	2
29	376	1
29	375	1
29	369	2
29	373	2
29	375	2
30	87	1
30	88	1
30	89	2
30	90	2
30	88	2
30	89	2
31	103.7	1
31	101.1	1
31	96.48	2
31	97.18	2
31	97.51	2
31	96.15	2
32	117.4	1
32	116.6	1
32	115.2	2
32	115.5	2
32	113.6	2
32	114.7	2
33	109.8	1
33	108	1
33	101	2
33	97.3	2
33	100.4	2
33	98.5	2
34	93.2	1
34	93.2	1
34	88.3	2
34	88.4	2
34	88.5	2
34	88.5	2
35	83	1
35	82	1
35	80	2
35	80	2
35	80	2
35	80	2
36	88	1
36	88	1
36	81	2
36	81	2
36	81	2
36	81	2
37	111.2	1
37	112.1	1
37	100	2
37	101.1	2
37	99.6	2
37	100.5	2
38	93.1	1
38	93	1
38	84.8	2
38	84.6	2
38	83.6	2
38	83.4	2
39	67	1
39	68	1
39	60	2
39	60	2
39	62	2
39	62	2
40	114.9	1
40	114.4	1
40	106.9	2
40	107.9	2
40	110.4	2

38

40	110.2	2
41	94	1
41	92	1
41	88	2
41	88	2
41	87	2
41	87	2
42	94.89	1
42	94.87	1
42	86.3	2
42	84.59	2
42	86.45	2
42	84.73	2
43	95.64	1
43	95.2	1
43	89.5	2
43	86.56	2
43	90.59	2
43	88.41	2
44	135.9	1
44	138.2	1
44	127.7	2
44	126.2	2
44	127.4	2
44	126.2	2
45	106.9	1
45	106.7	1
45	97.6	2
45	97.5	2
45	97.5	2
45	97.2	2
46	95	1
46	96	1
46	85	2
46	86.5	2
46	86	2
46	86	2
47	104.82	1
47	101.75	1
47	95.06	2
47	92.11	2
47	91.68	2
47	91.86	2
48	39.33	1
48	37.33	1
48	31.33	2
48	31.67	2
48	30.67	2
48	31.67	2
49	97	1
49	104	1
49	93	2
49	95	2
49	93	2
49	93.5	2
50	71	1
50	72	1
50	63	2
50	64	2
50	65	2
50	64	2
51	94.92	1
51	95.41	1
51	90.75	2
51	89.24	2
51	90.01	2
51	89.83	2
END		

Set 2:
lab2 is the lab identification for the direct measurement
meas2 is the direct SRM 46h measurement

lab2[]	meas2[]
1	365.2
2	403.6
3	371

4	362
5	352.9
6	377.1
7	363
8	361.1
9	360.6
10	354
11	349.9
12	353
13	368.6
14	361.6
15	360
16	365
17	368
1	364
2	407.3
3	366.7
4	367
5	355.6
6	377.1
7	359
8	361.1
9	354
10	353.6
12	352
13	368.6
14	359.5
15	361
16	363
17	369
1	363.1
2	407.4
3	355.4
4	359
5	358.4
6	374.8
7	363
8	358.6
9	360.2
10	353.3
11	352
12	355
13	368.6
14	359.5
15	360
16	363
17	368
1	362
2	406.4
3	373.2
4	362
5	358.7
6	379.5
7	363
8	363.6
9	364.4
10	355.3
11	358.2
12	352
13	366.4
14	360.5
15	360
16	363
17	368
END	

Data set 3:
lab3 is the lab identification for the direct SRM 114q measurement meas114 is the direct SRM 114q measurement

lab3[]	meas114[]
1	381.8
2	396
3	381.8
4	391
5	384.6
6	397.8
7	379

40

8	383
9	379.4
10	373.3
11	368.2
12	373
13	384
14	385.7
15	383
16	381
17	382
1	382.3
2	376
3	383.9
4	387
5	380.4
6	400
7	380
8	387.7
9	380.6
10	373.6
11	368.2
12	371
13	384
14	383.8
15	383
16	382
17	382
END	

Appendix C: Questionnaire for participants

Note: Underlined and in bold the values that were assigned by NIST

SECTION A: Laser Diffraction (wet): specimen dispersed in a liquid

Device brand and model:

_____

_____

Parameters to use (mandatory)
➢ Medium: **Isopropanol (IPA)**

    Is this the medium that you normally use (circle one):   Yes   No

    If no, please specify what you normally use: _____

_____

➢ Complex refractive index used for powder: Real: **1.7**   Imaginary: **1.0**

➢ Refractive index (real) used for medium: **1.39**

➢ Do not use a surfactant

Some information on your method
➢ Concentration of the dispersion: [g/mL] _____ (if known)

       Diluted from more concentrated stock? YES NO

       If yes, give stock concentration [g/L]: _____

- Note: use particle density of 3.2 g/mL for calculation of solids concentration. Also indicate density used for medium [g/mL]: _____

➢ Ultrasonication of sample suspension (circle one):   Yes   No

    If yes, please specify intensity and duration: _____

_____

➢ Was ultrasonic treatment performed (circle one):

    (a) inside PSD device;   (b) prior to introduction into device;   (c) both

- If (b) or (c), please identify type of external ultrasonicator used (circle one)

               bath   submersible horn

- If (b) or (c), was the external ultrasonication performed on a (circle one)

           concentrate or   dilute dispersion*

*refers to a suspension at or near the solids concentration used in the actual measurement

Test and results:
➢ Duration of the measurement in the PSD device [sec]: _____

➢ Model used to interpret the results: (circle one): Mie   Fraunhofer   Both

Notes: (add any information that could be useful to better describe the procedure used):

SECTION B: Laser Diffraction (Dry): specimen dispersed in air

Device brand and model:

Parameters to use (mandatory)
➢ Complex refractive index used for powder: Real: **1.7** Imaginary: **1.0**

Particle dispersion:
➢ Dispersion procedure: (circle one)   compressed air   vacuum

If compressed air, pressure setting used [bar]

Test and results:
➢ Duration of the measurement in the PSD device [s]:

➢ Model used to interpret the results: (circle one):   Mie   Fraunhofer   Both

Notes: (add any information that could be useful to better describe the procedure used):

Appendix D: Data received from the Round-robin for PSD

Table D.1: Data for SRM 114q by LD-D

Size [μm]	Cumulative Particle size distribution by Laboratory (CCRL Code) [%]												
	142	156	178	180	219	255	309	504	1323	2491	2522	2763	3255
1	6.62	3.70	3.44	11.29	5.25	6.32	4.2	5.96	4.48	5.30	1.50	5.54	3.41
1.5	9.84	7.02	6.29	14.24	8.24	8.02	7.2	8.79	6.93	8.47	4.55	8.54	6.81
2	12.74	10.28	9.13	17.18	10.71	10.20	10.3	11.62	9.41	11.53	7.86	11.39	10.03
3	18.14	16.38	14.81	22.77	14.95	13.72	16.3	16.71	14.46	17.30	13.85	16.89	15.27
4	23.03	21.62	19.39	27.90	18.58	17.17	21.9	21.27	19.34	22.45	18.93	21.98	19.55
6	31.52	30.20	28.56	36.71	25.18	23.80	31.3	28.99	28.07	31.17	27.20	30.83	26.76
8	39.01	37.40	36.69	44.15	31.28	30.26	39.2	35.63	35.75	38.73	34.58	38.47	33.15
12	52.61	50.14	48.43	57.69	42.22	42.53	53.4	47.69	49.40	52.15	48.02	51.67	45.37
16	64.54	61.33	57.72	70.33	53.25	53.93	65.9	58.76	61.15	63.55	59.99	62.92	57.00
24	82.11	78.40	76.28	89.14	73.59	72.86	84.6	76.73	78.62	80.03	77.85	79.57	76.68
32	92.11	88.56	91.89	97.49	86.27	85.08	94.6	88.46	89.07	89.63	88.68	89.74	89.01
48	99.36	96.72	99.14	100.00	95.04	95.72	99.8	98.35	97.78	97.73	97.81	98.04	97.37
64	100.00	98.50	99.65	100.00	97.53	98.99	100.0	100.00	99.79	99.74	99.86	99.88	98.05
96	100.00	98.74	100.00	100.00	99.03	99.98	100.0	100.00	100.00	99.98	100.00	100.00	98.11
128	100.00	98.74	100.00	100.00	99.63	100.00	100.0	100.00	100.00	99.98	100.00	100.00	98.89

Table D.2: SRM 114 d by LD-W

Size [μm]	Cumulative Particle size distribution by Laboratory (CCRL Code) [%]				
	94	126	343	605	1079
1	13.37	4.55	1.14		4.78
1.5	16.05	7.08	3.42	0.99	8.64
2	18.73	9.57	5.70	2.57	12.24
3	23.72	14.54	10.70	7.18	17.99
4	28.21	19.43	15.41	12.28	22.76
6	36.24	28.48	23.77	22.30	31.13
8	43.56	36.43	31.31	31.49	38.27
12	56.67	50.00	44.71	43.84	50.42
16	67.99	61.69	56.88	54.48	61.93
24	84.33	79.91	75.98	78.67	81.13
32	93.24	90.69	87.90	92.83	91.63
48	99.52	97.41	97.77	98.78	98.48
64	99.99	98.41	99.94	99.77	99.71
96	99.99	99.58	100.00	100.00	99.99
128	99.99	99.93	100.00	100.00	100.00

Table D.3: SRM 46h by LD-D

Size [μm]	Cumulative Particle size distribution by Laboratory (CCRL Code) [%]													
	142		156		178		180		219		255		309	
1	6.86	6.76	3.59	3.57	3.63	3.58	11.59	11.15	5.06	5.28	6.54	6.75	4.21	4.07
1.5	10.19	10.02	6.75	6.71	6.54	6.49	14.63	14.13	7.91	8.21	8.26	8.53	7.26	7.08
2	13.16	12.91	9.81	9.76	9.46	9.40	17.70	17.13	10.27	10.64	10.45	10.81	10.27	10.04
3	18.48	18.10	15.42	15.35	15.29	15.21	23.28	22.63	14.24	14.81	13.91	14.42	16.07	15.75
4	22.96	22.52	20.18	20.10	19.66	19.53	28.07	27.40	17.54	18.28	17.22	17.88	21.26	20.83
6	29.95	29.56	27.75	27.68	28.42	28.18	35.96	35.31	23.17	24.15	23.26	24.25	29.94	29.22
8	35.52	35.23	33.73	33.67	35.83	35.55	42.37	41.77	28.20	29.29	28.77	30.09	37.07	35.87
12	45.23	45.11	43.32	43.27	45.60	45.38	52.95	52.48	36.98	38.04	38.59	40.45	48.96	46.33
16	54.08	54.04	51.18	51.11	52.99	52.89	61.95	61.65	44.80	45.75	47.59	49.82	59.14	54.97
24	69.07	69.09	63.88	63.74	67.76	67.90	76.68	76.69	58.78	59.52	63.96	66.45	75.33	69.31
32	80.12	80.06	73.41	73.20	80.99	81.26	87.09	87.25	70.30	70.80	76.67	78.94	85.83	79.85
48	92.97	92.66	85.39	85.03	93.05	93.08	97.37	97.52	85.02	85.21	90.95	92.37	95.47	91.54
64	98.29	97.96	91.43	90.98	96.96	96.97	99.81	99.85	91.92	91.97	97.00	97.60	98.46	95.89
96	100.00	99.99	95.84	95.36	99.99	100.00	100.00	100.00	96.58	96.56	99.82	99.88	99.54	97.46
128	100.00	100.00	96.78	96.31	100.00	100.00	100.00	100.00	98.19	98.16	100.00	100.00	99.55	97.48

Size [μm]	Cumulative Particle size distribution by Laboratory (CCRL Code) [%]										
	504		1323		2491		2522		2763		3255	
1	6.08	5.88	4.49	4.63	5.50	5.58	1.99	1.99	5.54	5.50	3.66	3.66
1.5	8.93	8.64	6.93	7.19	8.74	8.89	5.40	5.40	8.55	8.47	7.31	7.31
2	11.78	11.40	9.34	9.70	11.83	12.04	9.04	9.04	11.40	11.29	10.72	10.72
3	16.82	16.24	14.17	14.73	17.55	17.89	15.68	15.68	16.81	16.61	15.93	15.93
4	21.13	20.43	18.75	19.45	22.52	22.98	21.36	21.36	21.69	21.40	19.86	19.86
6	27.67	26.91	26.65	27.54	30.53	31.18	30.29	30.29	29.69	29.22	26.08	26.08
8	32.58	31.78	33.13	34.15	36.99	37.75	37.72	37.72	36.06	35.44	31.33	31.33
12	40.85	39.77	43.69	44.90	47.62	48.37	49.32	49.32	46.20	45.39	41.14	41.14
16	48.55	47.21	52.42	53.80	56.28	56.90	58.42	58.42	54.62	53.71	49.92	49.92
24	62.25	60.76	66.32	67.95	69.45	69.76	71.62	71.62	67.85	66.90	64.69	64.69
32	73.12	71.52	76.35	78.18	78.53	78.68	80.69	80.69	77.24	76.44	76.14	76.14
48	87.10	85.09	88.28	90.36	89.10	89.26	91.42	91.42	88.01	87.54	89.63	89.63
64	94.52	92.56	93.96	96.02	93.85	94.25	96.51	96.51	93.13	92.79	94.88	94.88
96	99.77	99.03	98.05	99.57	96.35	97.16	99.64	99.64	96.48	96.07	97.40	97.40
128	100.00	100.00	99.09	99.95	96.48	97.33	100.00	100.00	96.93	96.48	98.39	98.39

Table D.4: SRM 46h by LD-W

Size [μm]	Cumulative Particle size distribution by Laboratory (CCRL Code) [%]									
	94		126		343		605		1079	
1	14.06	13.64	4.87	4.82	1.29	1.33			5.53	5.67
1.5	16.61	15.93	7.17	7.06	3.56	3.53	1.28	1.26	9.71	10.00
2	19.26	18.46	9.48	9.27	5.82	5.73	2.99	2.97	13.49	13.91
3	24.30	23.56	14.36	13.87	11.02	10.94	7.89	7.87	19.36	19.89
4	28.74	28.20	19.35	18.56	15.89	15.87	13.32	13.29	24.18	24.75
6	36.23	36.00	28.58	27.31	24.12	24.25	23.05	23.04	32.07	32.74
8	42.47	42.40	36.30	34.79	30.89	31.10	31.18	31.20	38.41	39.14
12	52.79	52.80	48.25	46.70	41.70	41.96	42.16	42.19	48.75	49.54
16	61.29	61.26	57.48	56.08	51.15	51.41	50.50	50.51	57.43	58.39
24	74.71	74.49	71.30	70.16	65.97	66.20	66.67	66.67	71.51	72.69
32	84.12	83.75	80.96	79.97	77.01	77.20	79.50	79.46	81.49	82.48
48	94.45	94.05	91.76	90.78	90.14	90.28	92.06	91.91	92.32	92.92
64	98.42	98.20	95.94	94.89	95.99	96.08	96.44	96.37	96.19	96.63
96	100.00	100.00	99.06	97.81	99.49	99.51	98.83	98.79	98.44	98.76
128	100.00	100.00	99.80	98.88	100.00	100.00	99.67	99.65	99.01	99.27